Excitation of periodic magnetic field oscillations in the ULF range by amplitude modulated HF waves

A.-A. MAUL (*), M. T. RIETVELD (**), P. STUBBE, and H. KOPKA

Max-Planck-Institut für Aeronomie, Postfach 20, D-3411 *Katlenburg-Lindau, F.R.G.*

Received February 7, 1990; revised June 21, 1990; accepted July 3, 1990.

ABSTRACT. High power HF radio waves radiated into the ionosphere strongly enhance the electron temperature. This electron heating can cause perturbations in the conductivity tensor *via* an enhancement of the collision frequency or the electron density, depending on the modulation frequency of the HF wave. The periodically altered conductivities result in an ac current that emits electromagnetic waves. Two experiments with modulation frequencies between 0.7 and 9 Hz, and one with frequencies of 1425 Hz, 1 Hz, and 8.33 mHz are studied in detail and compared with numerical calculations. It is found that ellipticity and orientation of the polarization ellipse of the measured magnetic wave field can be ascribed to the effects of the temperature and density modulation.

Annales Geophysicae, 1990, **8,** (11), 765-780.

1. INTRODUCTION

The radiation of high-power HF waves into the ionospheric plasma at various locations and the investigation of the connected physical effects have been a fruitful field of research for almost thirty years (see e.g. Gurevich and Migulin, 1982). One area which has received much attention by several groups is the modulation of ionospheric conductivities and currents in the lower ionosphere (Gul'el'mi *et al.*, 1985; Lunnen *et al.*, 1985; Stubbe *et al.*, 1985). In recent years numerous papers have dealt with the generation of VLF and ELF waves by means of the Max-Planck-Institut für Aeronomie's Heating facility near Tromsø in northern Norway. This region is particularly suitable for such experiments due to the presence of the auroral electrojet, because the modification of this ionospheric current causes stronger effects than the modification of currents generated by atmospheric tides in lower latitudes. A comprehensive description of the Heating facility is given in the report of Stubbe and Kopka (1979). The VLF/ELF waves excited by the ionospheric heating have been measured on the ground near the source (Rietveld *et al.*, 1987, 1989), and hundreds of kilometres away from the source (Barr *et al.*, 1986). Their findings show that these waves can be fed and ducted in the waveguide confined by ionosphere and earth. The modelling of the characteristics of these waves under various geophysical conditions give evidence that the waves in the frequency range above a few hundred Hertz are excited by modulation of the electron temperature.

The periodic changes of the electron temperature lead to corresponding changes of the electron collision frequency and to a periodic alteration of Hall and Pedersen currents. Therefore an artificial ac current is superposed on the existing dc current. According to Ohm's law, the ac current is directly related to the ionospheric electric field. The magnetic field of the ELF wave radiated by the ac current can be measured on the ground and exhibits amplitudes up to several picotesla.

On lowering the modulation frequency to ultralow frequencies (ULF), two other effects occur. First, the distance from the source current to the observation site becomes shorter than the wavelength and thus the magnetic field of the current distribution is measured instead of that of the wave. Secondly, the electron density modulation due to the inverse temperature dependence of the recombination coefficients of the O_2^+ and NO^+ ions appears. The characteristic time for this process (called density relaxation time) is of the order of seconds and hence only measurable at frequencies lower than some Hertz. This is the dominant effect if the modulation period becomes larger than the density relaxation time.

Few results have been published of experiments with modulation frequencies below several hundred Hz since the first observations of artificial 3.1 Hz mag-

(*) Now at: Alfred-Wegener-Institut für Polar- und Meeresforschung, Am Handelshafen 12, D-2850 Bremerhaven, FRG.
(**) Present address: EISCAT, N-9027 Ramfjordbotn, Norway.

netic perturbations produced by a HF transmitter reported by Getmantsev *et al.* (1977). Results of ULF modulation experiments from the Tromsø heater, including preliminary measurements in the Hz range, have been briefly summarized by Stubbe *et al.* (1985) and references therein, but so far no quantitative analysis has been made.

Now we present and analyze in detail the data from three experiments. The first two deal only with modulation frequencies between 0.7 and 9 Hz. In this frequency range changes of the collision frequency and density can contribute comparable amounts to the ULF magnetic field depending on the height in which the energy of the heating wave is deposited. The superposition of these two effects seriously complicates data analysis so that no systematic examinations of the polarization characteristics of the observed magnetic field perturbations or model calculations for them have been made up to now.

Fortunately the two disturbances influence the conductivity tensor with different signs leading to currents with different phases. Consequently the polarization ellipse of the magnetic field vector exhibits an elliptical form if the heating wave reaches such heights where considerable density changes are possible. This effect is thought to be operative only at heights above 85 km since at lower heights water cluster ions, which after Huang *et al.* (1978) have recombination coefficients with very little temperature dependence, are abundant. Without density modulation the ellipse degenerates to a linear form. The orientation of the polarization ellipse with respect to the ionospheric electric field is determined by the ratio of Hall and Pedersen current perturbations. The strength and direction of the electric field is derived from data of the STARE and the EISCAT facilities. We will attempt to show that our observed variations of the ellipse parameters can be explained by the different heating wave polarizations and the different ionospheric conditions pertaining at the time of our experiments.

The third experiment differs from the other two since ELF measurements with modulation frequencies of 1425 Hz and ULF measurements with periods of 1 s and 120 s were carried out simultaneously, thus allowing the two different excitation processes to be compared.

2. EXPERIMENTAL RESULTS

2.1. Experimental set-up

The magnetic field oscillations are measured with induction coils at Lavangsdalen 18 km south of the Heating facility in Ramfjordmoen. The two orthogonal coils are oriented in the horizontal geomagnetic H (northward) and D (eastward) directions. These directions are almost identical with geographic north and east because of the low declination of approximately 0.5 degrees east near Tromsø. The frequency range of the sensor unit is limited to high frequencies by a low pass filter (cut-off frequency 35 Hz) and to about 0.1 Hz at low frequencies. The system has its maximum sensitivity at 10 Hz. Two UHF carrier waves are modulated with the low pass filtered signals and sent to the Heating site, where, after the demodulation, the digital recording onto floppy disks takes place. The sample rate of the recording unit can be freely chosen to be suitable for the applied modulation frequency, the only restriction being that the sample period has to be above 1.6 ms. If desired, ELF/VLF data can be sent over the same link to Ramfjordmoen and after a different processing they can be stored on the same disks, so that simultaneous measurements of VLF/ELF and ULF frequencies are possible.

2.2. The magnetic background during the experiments in October and November 1984

In 1984 and 1985 many ULF experiments were performed with the Heating facility and the three most successful ones are described in this paper. Two measurements took place on 7th and 8th of November, 1984 during a magnetic storm. The first was conducted shortly after the beginning of the storm and the form and orientation of the polarization ellipses show fast changes according to variations of the electron density profile and direction of the ionospheric electric field. The second experiment was performed throughout rather constant conditions in the recovery phase of the storm. The last experiment presented in this paper was carried out on October 26, 1984 during a period of very low magnetic activity.

Figure 1 displays two magnetograms of the flux gate magnetometer at Kilpisjärvi, 87 km southeast of the Heating facility, for the time intervals from 16 to

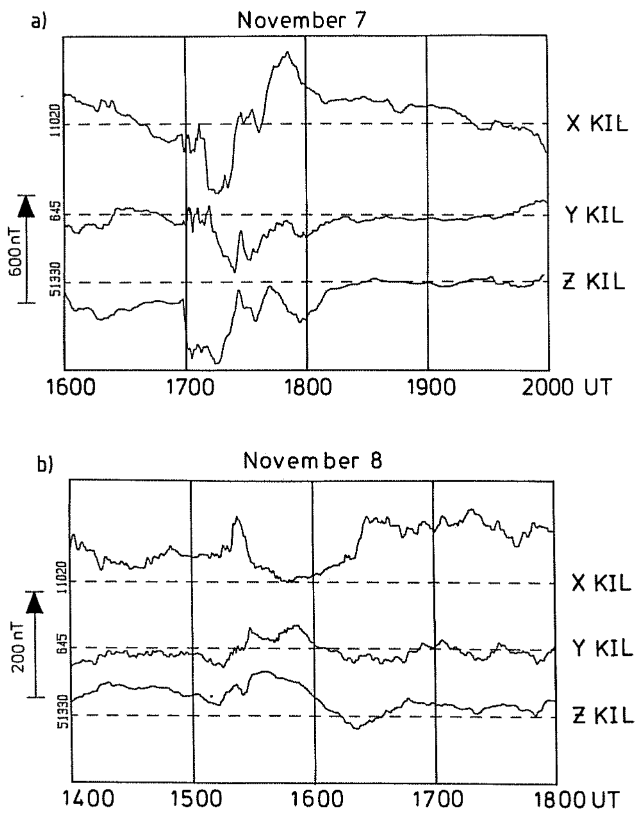

Figure 1
Magnetograms of the flux gate magnetometer at Kilpisjärvi covering the time intervals of the two experiments. (a) 7.11.84, 1600-2000 UT, (b) 8.11.84, 1400-1800 UT.

20 UT on November 7 and from 14 to 18 UT on November 8. They cover the two experiments, which were performed between 1719 and 1804 UT on November 7 and from 1602 to 1659 UT on November 8. The recording system at Kilpisjärvi is part of the « EISCAT magnetometer cross » operated jointly by the Finnish Meteorological Institute, the Sodankylä Geophysical Institute and the Geophysical Institute of the Technical University of Braunschweig. The magnetometers are oriented in geographical directions, X pointing northward. The upper magnetogram shows 4 h of data recorded shortly after the beginning of a magnetic storm around 15 UT. This storm was responsible for the magnetic disturbances on these two days. Notice that the scaling factor for November 8 is three times larger than for November 7 because of the decrease of magnetic activity. The X component shows the largest disturbances indicating that the variations are caused by the mainly east-west flowing auroral electrojet. Because of the lower activity on November 8 the conditions are more homogeneous, so the experiment on this day is considered first.

2.3. Experiments of November 8, 1984

Table 1 shows the program of the measurements and some parameters of the heating operation on November 8. Between 1602 and 1630 UT x-mode (left hand polarization) was used and from 1632 until 1659 UT o-mode heating. The carrier was square-wave modulated, the sequence of the modulation frequencies being displayed in the right part of Table 1. Each frequency was used for 2 min, so a whole cycle lasted 14 min. After two cycles the mode was changed, during the 2 min between 1630 and 1632 UT. At 1632 UT the program was continued starting with the modulation frequency of 3.84 Hz until the program ended at 1659 UT.

Good STARE data were available for November 7 and 8 because the electric field exceeded the threshold value of approximately 15 mV/m, required for excitement of the instabilities, over a large range of latitudes due to the enhanced magnetic activity.

Figure 2 shows the electron flow pattern at 19 degrees east as a function of universal time and geographic latitude using an integration time of 60 s. The geographic latitude of the Heating facility (69.6° N, 19.2° E) is marked by an arrow. The profile shows generally westward directed electron drift velocities, corresponding to an eastward electrojet as one would expect for this local time. In the heated region the velocities reach roughly 1700 m/s at first and get a small southward component at 1613 UT. Between

Table 1
Parameters of the Heating experiments on November 8.

Time interval [UT]	Polarization	Radiated power [MW]	Carrier frequency [MHz]	Cycle of modulation frequencies (2 min for every frequency) [Hz]
1602-1630	x-mode	241	2.759	0.7 3.84 1.07 5.88 1.64 9.0 2.51
1632-1659	o-mode			

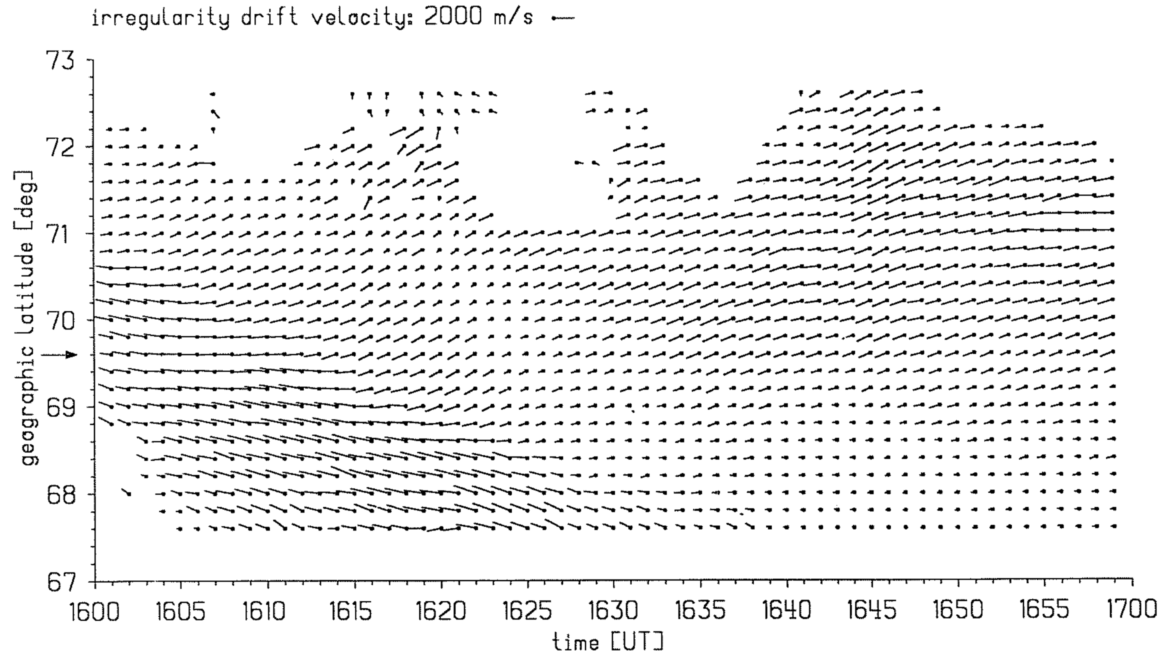

Figure 2
Phase velocities of 1 m *plasma waves as observed by the* STARE *radar between* 1600 *and* 1700 UT *on November* 8 *for a latitude profile along* 19° *eastern longitude using an integration time of* 60 s. *The arrows point away from the dots. The geographic latitude of the Heating facility is indicated by an arrow.*

1622 and 1627 UT they decrease to their minimum value of 400 m/s, after which they rise to 1200 m/s for the rest of the experiment. The corresponding ionospheric electric field fluctuates between 20 and 85 mV/m with a mean value of about 50 mV/m.

Figure 3 exhibits an example of the magnetic pulsations recorded at the modulation frequency of 3.84 Hz for a time interval of 10 s. In the upper part the data are shown high pass filtered with a cut-off period of 10 s. The signal is superposed on the long-period background with higher amplitudes. The lower part shows the high pass filtered data whose cut-off period is 1 s. The vertical lines are intended to facilitate the tracing of the magnetic field oscillations. They include four cycles of 3.84 Hz which are well developed in the northward component and less in the eastward component. Notice the amplitude difference between the long-period background and the signal of about one or two orders. This does not matter at frequencies greater than 1 Hz but for modulation frequencies of 1 Hz or lower the background masks the artificial magnetic field oscillations. At frequencies greater than 1 Hz however noise at the Schumann resonance frequencies can become a problem.

The typical form of the oscillations is obtained by stacking the cycles which eliminates aperiodic signals and oscillations at other periods. The result for the modulation frequency of 3.84 Hz during the interval from 1604 to 1606 UT is shown in Figure 4. The values fluctuate around zero due to centering of the data, with the error bars indicating the errors of the mean values. Figure 4 shows that the amplitude in the H component (2.1 pT) is about twice that in the D component (1.0 pT) and that there are smaller errors in H than in D as one would expect from Figure 3. The flanks of the curves display a slow rise and fall with time caused by the low pass filter in the recording unit.

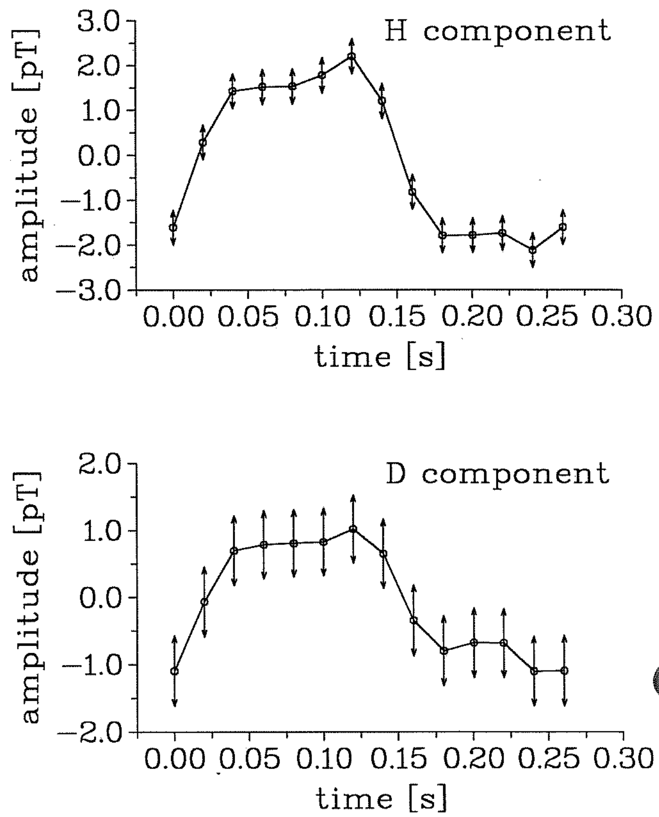

Figure 4
Typical form of the oscillations obtained after stacking 460 *cycles of the modulation frequency of* 3.84 Hz *recorded between* 1604 and 1606 UT *on November* 8.

Figure 5 shows the amplitude spectra of the two time series. Prominent peaks at the fundamental frequency of 3.84 Hz and the corresponding odd harmonics (11.5 and 19.2 Hz) are marked by arrows. The peaks seen at 16 2/3 Hz are caused by an electrified railway

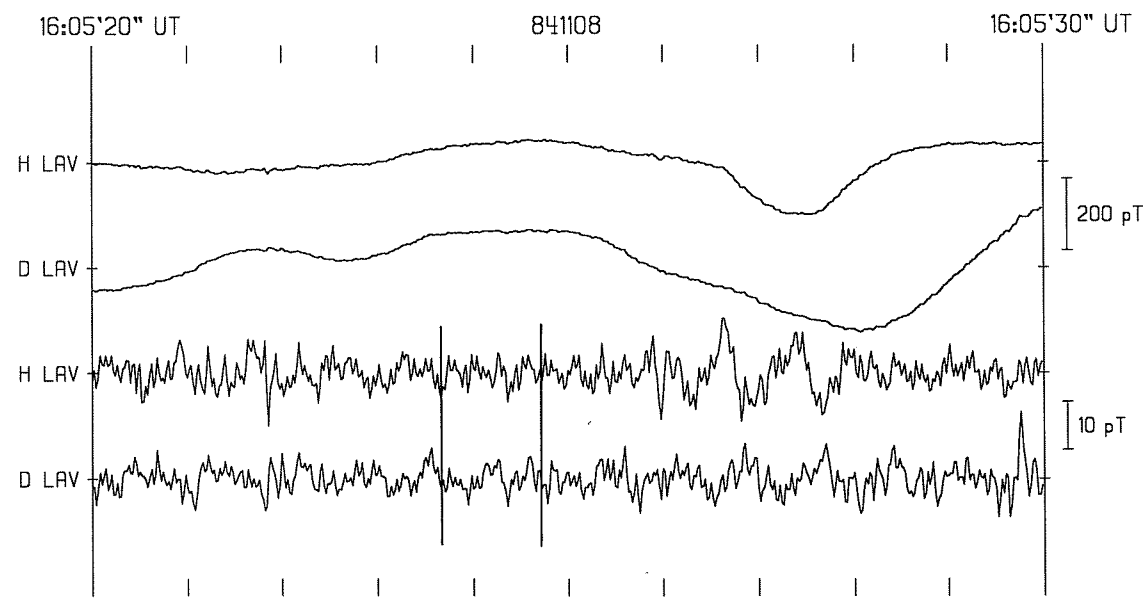

Figure 3
Recording example of the induction coils for the heating experiments on November 8 *displaying the time interval between* 16 : 05′ 20″ and 16:05′ 30″ UT. *Upper two rows : high pass filtered H and D component (cut-off period :* 10 s*). Lower two rows : high pass filtered data (cut-off period :* 1 s*). The vertical bars include four cycles of the modulation frequency of* 3.84 Hz.

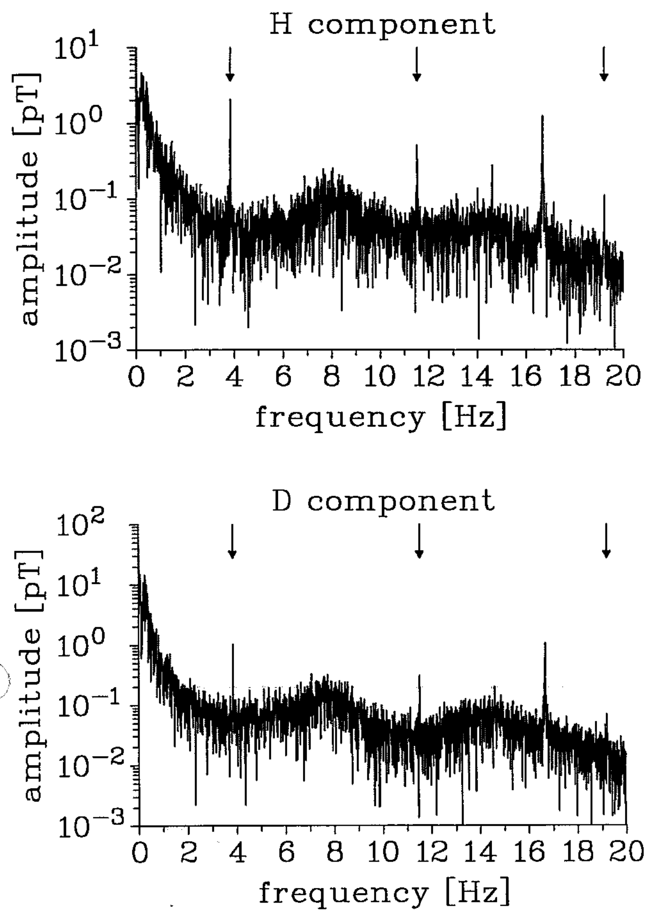

Figure 5

Amplitude spectra of the magnetic H and D components for the same time interval as in Figure 4. The fundamental frequency of the artificial oscillations and the corresponding odd harmonics are marked by arrows.

from Kiruna to Narvik, which is roughly 134 km away from the recording site. The first and second harmonic of the Schumann resonances at about 8 and 15 Hz are also discernable as broad maxima.

The magnetic field polarization parameters are obtained from auto and cross spectra of the two components (Rankin and Kurtz, 1970). The disturbance vector is elliptical in the horizontal plane, if only one distinct frequency is considered. This ellipse is characterized by four parameters. The first parameter, the degree of polarization, is defined as the ratio of the intensity of the polarized signals to the total intensities of the signal and the unpolarized noise. The degree of polarization defines the quality of the three other parameters: ellipticity, orientation of the ellipse and sense of rotation. Because of the simultaneous occurrence of the higher harmonics, we have data covering a wide frequency interval. The normalized polarization ellipses for the fundamental frequency as well as the odd harmonics are plotted vertically in Figure 6 for each 2 min time interval. (To facilitate comparisons of ellipticity and orientation of the ellipses to be made the major half-axes have all been normalized to the same length). The number plotted to the left of the ellipse is the frequency. The ellipses are oriented such that magnetic north is directed upwards and magnetic east to the right. The arrow showing the sense of rotation is omitted if the ellipse has a nearly linear form. If the degree of polarization is less than 0.5, and therefore noise is dominant, it is marked by an asterisk above the frequency. The electron flow pattern as measured by STARE shows that the ionospheric electric field changes only a little in direction. A corresponding behaviour is seen in the

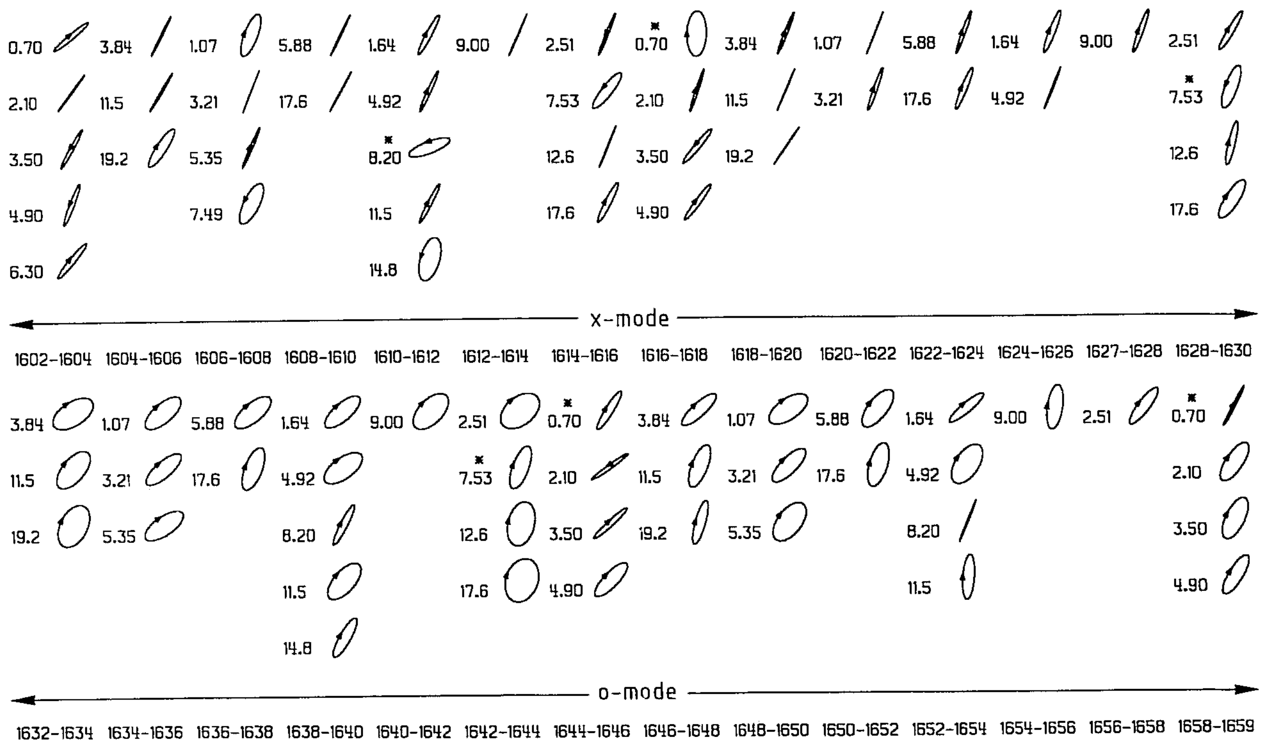

Figure 6

Normalized polarization ellipses of the fundamental frequencies and their odd harmonics (if discernible) for the whole experiment on November 8. Upper half: x-mode heating, lower half: o-mode heating. Below each column: analyzed time interval, left of each ellipse: oscillation frequency. Ellipses with a degree of polarization less than 0.5 are marked by asterisks. The rotation sense of the magnetic disturbance vector is indicated by an arrowhead on those ellipses which are not linearly polarized.

polarization ellipses which have all similar orientations, with differences occurring only if the ellipses have a low degree of polarization. As mentioned above, this occurs at frequencies of 0.7 Hz because of the higher amplitudes of the background and at frequencies around 8 Hz where the Schumann resonances have larger amplitudes than the signals generated by heating. The ellipses in each column are very similar, showing that there is little frequency dependence in the frequency interval from 0.7 to 19.2 Hz. The sense of rotation is generally clockwise, only very narrow ellipses or those with a low degree of polarization showing a contrary sense of rotation.

By close inspection of Figure 6, two systematic differences can be recognized between the ellipses in the upper and lower halves. First, the polarization is nearly linear in case of x-mode heating and elliptical for o-mode heating. Second, the orientation of the x-mode ellipses is rotated by an angle of 20° to 30° to that of the o-mode ellipses.

Figure 7 shows the ellipse orientation of the fundamental oscillation compared with the direction of the ionospheric electric field, derived from the STARE electron velocity vectors — now with true amplitudes contrary to the normalized ellipses in Figure 6. If only ellipses without asterisks are taken into account, the angle between the major half-axis and the electric field, ϕ_0 has a mean of 40° for x-mode heating and a mean of 64° for o-mode heating. The length of the major half-axis, and hence the intensity of the artificial current, varies as the strength of the ionospheric electric field. Thus it appears legitimate to assume that the current disturbance is proportional to the ionospheric electric field. Generally, the fundamental oscillations have amplitudes between 1 and 3 pT.

2.4. Experiments of November 7, 1984

Table 2 lists the details of the measurements on November 7. Between 1719 and 1728 UT o-mode heating and between 1729 and 1732 UT x-mode heating took place with a modulation frequency of 3 Hz. Then the modulation frequency was cyclically altered for the next 32 min as on November 8, but

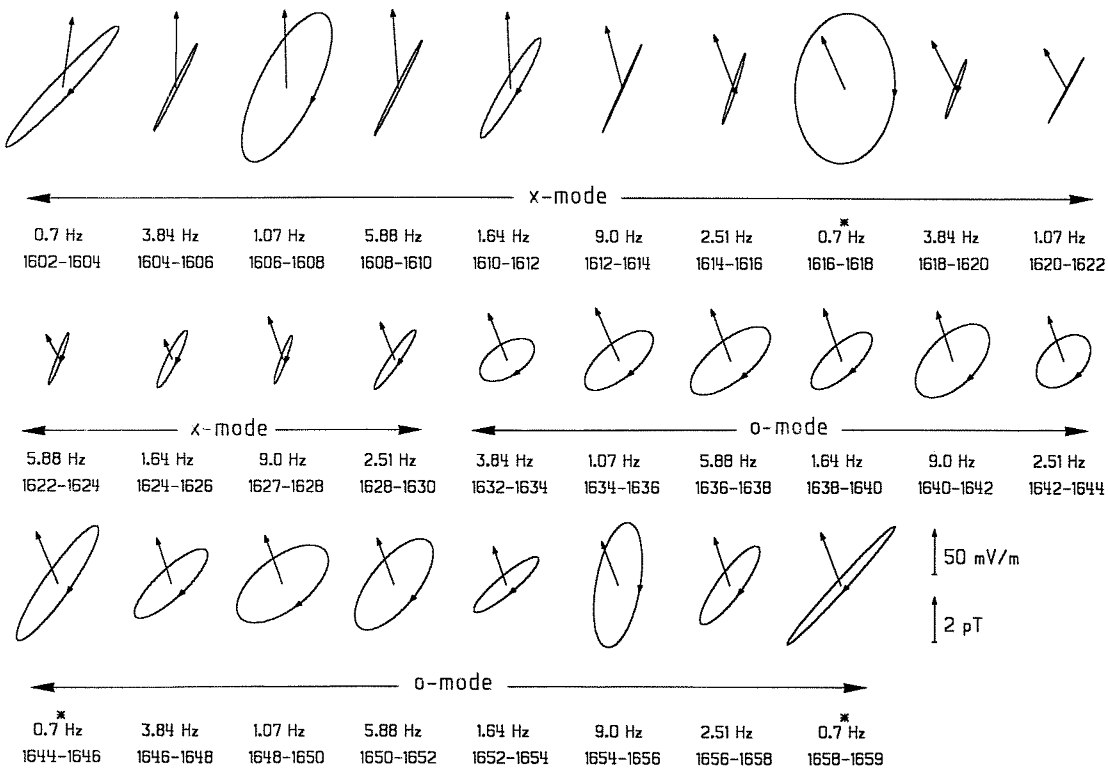

Figure 7
Polarization ellipses of the fundamental frequencies with true (not normalized) amplitudes for the experiments on November 8 together with the ionospheric electric field vector derived from the STARE data.

Table 2
Parameters of the Heating experiments on November 7.

Time interval [UT]	Polarization	Radiated power [MW]	Carrier frequency [MHz]	Modulation frequency [Hz]
1719-1728 1729-1732 1732-1804	o-mode x-mode x-mode	241	5.423	3 3 0.7 1 2 3 5 7 9

with slightly different frequencies. Again each frequency was used for 2 min. The recording began at 1721 UT, so no data were acquired for the first 2 min.

Corresponding to the disturbed magnetic background (see Fig. 1) the STARE data in Figure 8 show a complex electron flow pattern at the beginning of the experiment. The drift velocities change their direction from eastward to westward at 1725 UT. At the same time the velocities increase from 500 m/s to 1500 m/s. In spite of a transient southward flow between 1735 and 1740 UT, the direction and magnitude of the drift velocity remained essentially the same for the rest of the experiment.

Figure 9 displays the normalized polarization ellipses in the same manner as Figure 6. Similar to the experiment on November 8, the ellipses of the odd

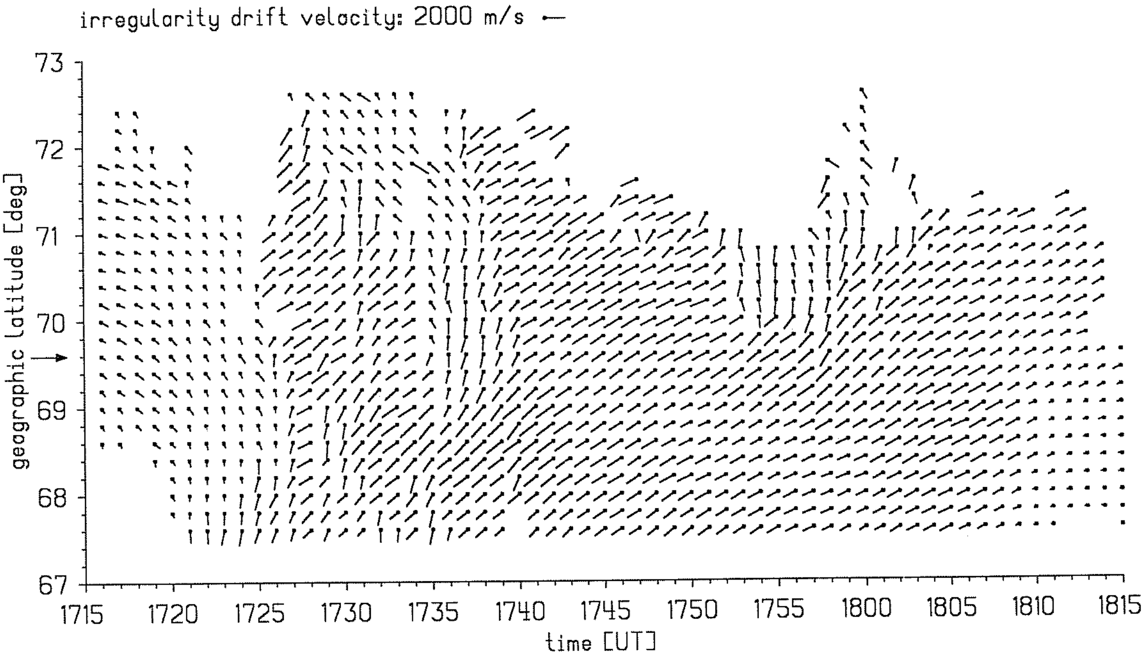

Figure 8
Phase velocities measured by STARE *between* 1715 *and* 1815 UT *on November* 7.

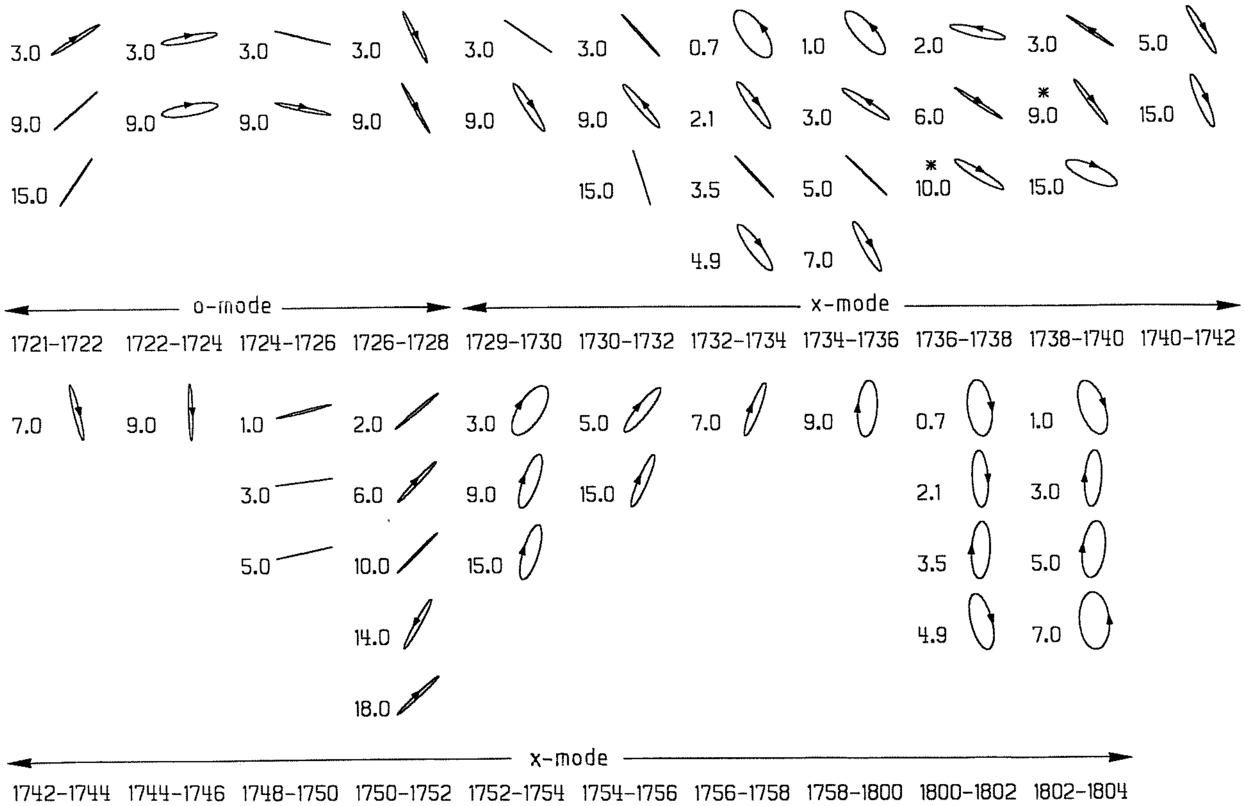

Figure 9
Normalized polarization ellipses of the experiments on November 7 *displayed in the same way as in Figure* 6.

harmonics have identical orientations to that of the fundamental frequency. Because of the dynamic changes in the ionosphere the ellipses have no constant orientation, but rotate by about 180° during the experiment. The form of the ellipses is nearly linear at the beginning of the measurements, with only ellipses at low modulation frequencies deviating from that form because the signals of their D components disappear in the noise. The ionospheric conditions change at 1752 UT, when the polarization ellipses lose their linear form. Nearly all ellipses have a right-hand sense of rotation, the only exceptions being when the oscillations are almost linearly polarized or at very low modulation frequencies.

More details can be recognized in Figure 10, where the ellipses of the fundamental frequencies are plotted together with the ambient ionospheric electric field deduced from the STARE data. The electric field is generally very strong with a maximum value of 85 mV/m at 1756 UT. The amplitudes are of the same order of magnitude as in the experiments on November 8. In case of *o*-mode heating (first four ellipses) ϕ_0 has a mean of 14° but after changing the polarization to *x*-mode, ϕ_0 decreases to 2° if only ellipses between 1729 and 1742 UT are considered and modulation frequencies of 0.7 and 1 Hz are omitted. Then the angle ϕ_0 increases to an average of 74° over the time interval from 1748 to 1800 UT.

2.5. Experiments of October 26, 1984

The experiments described in this section were performed from 1700 to 2118 UT and from 2217 to 2358 UT on October 26. They differ significantly from the two experiments presented above. First, the magnetic background was quiet, and second, the measurements made use of three completely different ELF and ULF modulation frequencies. For most of the time (24 min of half an hour) the carrier of 3.324 MHz was modulated with a period of 120 s (i.e. 1 min on, 1 min off) followed by a sequence of 1 min modulated with 1425 Hz, 1 min heater off and 1 min modulated with 1 Hz. A whole cycle lasted 30 min as displayed in Table 3. The three modulation frequencies cover a range of more than 5 orders so the different physical processes characteristic of each frequency can be clearly distinguished.

During a part of the experiment simultaneous EISCAT incoherent scatter radar measurements were performed, whereby the Tromsø antenna looked along the magnetic field line and the remote antennas pointed alternately to a common volume along the field line at heights of 109.5 and 171.5 km. Some of the results of the Heating and EISCAT experiments were already reported by Schlegel *et al.* (1987) who concentrated essentially on the EISCAT observations. In this paper we confine ourselves to the magnetic

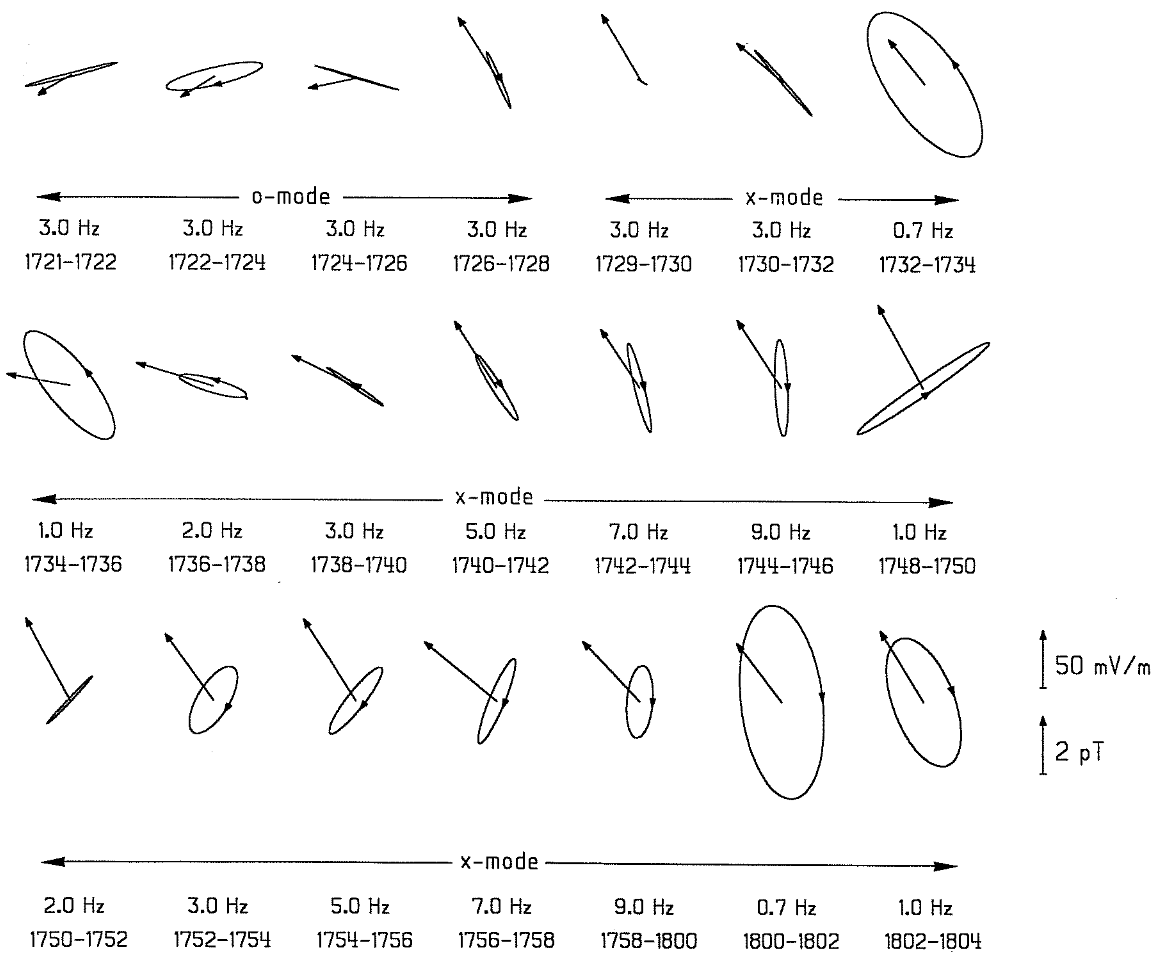

Figure 10
Polarization ellipses of the fondamental frequencies for the experiments on November 7 together with the ionospheric electric field vectors derived from the STARE *data.*

Table 3

Parameters of the Heating experiments on October 26. The cycle of the modulation frequencies has a duration of 30 min.

Time interval [UT]	Polarization	Radiated power [MW]	Carrier frequency [MHz]	Cycle of the modulation frequencies
1700-2118 2217-2358	*o*-mode	241	3.324	3 min : heater off, 24 min : 1 min heater on, 1 min heater off, 1 min : 1425 Hz, 1 min : heater off, 1 min : 1 Hz

field measurements (Fig. 8, Schlegel *et al.*, 1987) and make use of the EISCAT observations only to get an appropriate electron density profile and the ionospheric electric field from the drift velocities.

STARE measurements reveal that for a large time interval and over a wide latitudinal range the drift velocities do not reach the threshold for exciting observable instabilities due to the quiet conditions. Fortunately, a narrow latitude region south of Tromsø is an exception since Tromsø was for the most part of the experiment at the northern border of a quiet auroral arc, as shown by the all-sky-camera pictures taken every 2 min at Abisko. This aurora provided the *E*-layer near the Heating facility with precipitating particles and an ionospheric electric field which reached a maximum of about 50 mV/m.

Figure 11 displays the polarization ellipses for the three modulation frequencies together with the ionospheric electric field deduced from the EISCAT observations. In the top row the results of the 120 s-period experiments are plotted using the time intervals in which the signals had a reasonable signal to noise ratio. For the first time interval (1742 to 1757 UT) the spectrum analysis yielded a frequency of 7.14 mHz (period of 140 s) on account of phase jumps of the oscillations. For the other analyzed time intervals the prevailing frequency was determined to be 8.33 mHz (i.e. a period of 120 s) with maximum amplitudes in the order of about 1 nT.

The electric field vectors, which are derived from the EISCAT measurements at 171.5 km every 6 min, are the means for the analyzed time intervals except for the first one which is for 1801 UT. The electric field is directed to the north as expected at this local time. The angle ϕ_0 has a mean of $-71.6°$ (minus sign since major half-axis is anticlockwise with respect to the electric field vector), and the magnitude of the ellipses varies again with the strength of the electric field. The sense of rotation is again in all cases right-handed.

In the middle row are shown the polarization ellipses of the ten measurements made at 1 Hz (data gaps exist at 2129, 2159, and 2229 UT), together with the

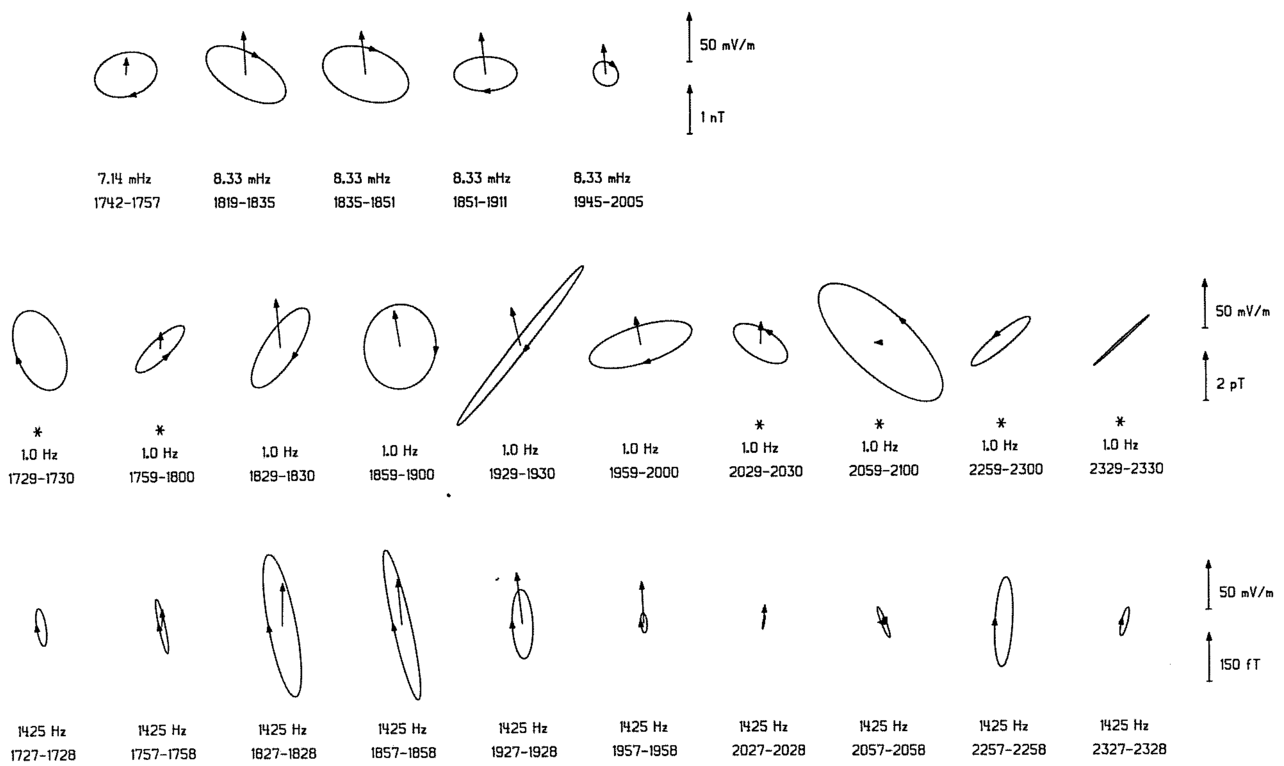

Figure 11

Polarization ellipses of the 120 s*-oscillations (top row),* 1 Hz*-experiments (middle row), and* 1425 Hz*-measurements (bottom row) together with the ionospheric electric field vectors derived from* EISCAT *data for October* 26.

electric field vectors recorded nearest in time, if such measurements existed. The ellipses marked by asterisks indicate a dominance of noise on account of the low amplitudes of the artificial oscillations, resulting from the low ionospheric electric field of less than about 20 mV/m. The ellipses show considerable variability in form and direction. For example, the ellipse at 1859 UT has approximately a circular shape but the next one, half an hour later, is nearly linear.

In contrast to the ULF experiments the ELF measurements with the modulation frequency of 1425 Hz show a remarkably homogeneous pattern ; only the oscillation amplitudes vary considerably. The maximum amplitude reaches the relatively small value of 0.17 pT, compared to amplitudes of about 1 pT or more under disturbed conditions reported earlier (Rietveld *et al.,* 1987). At first, the amplitudes change according to the strength of the ionospheric electric field, but decrease faster in the time interval between 1857 and 2057 UT. (For more details see Fig. 9 in the paper of Schlegel *et al.,* 1987). Two possible reasons for this behaviour are : first that the heated region and the line of sight of the EISCAT antenna in Tromsø do not coincide since the EISCAT antenna points slightly south of the modified area. Just at the time when the aurora moves further southward, the agreement between the amplitudes of the wavefield and the ionospheric electric field is re-established. A second reason could be the decrease in the *D*-region ionization after about 1945 UT shown in Plate 1 of Schlegel *et al.* (1987). All ellipses have a similar ellipticity of 0.19 (mean ratio of right- to left-handed rotating disturbance), and the major half-axes point roughly in the direction of the ionospheric electric field.

3. INTERPRETATION OF EXPERIMENTAL RESULTS

3.1. Theoretical background

The first part of the model, which calculates the conductivity perturbations and hence primary source currents as a function of height from 30 to 140 km in 0.5 km steps for a given modulation frequency, is described by Rietveld *et al.* (1986, 1987, 1989). Both the electron temperature and electron density modulation change the conductivity tensor according to

$$\Delta\boldsymbol{\sigma} = \left(\frac{\partial \boldsymbol{\sigma}}{\partial \nu}\frac{\mathrm{d}\nu}{\mathrm{d}T_e} + \frac{\partial \boldsymbol{\sigma}}{\partial N_e}\frac{\mathrm{d}N_e}{\mathrm{d}T_e} \right) \Delta T_e , \tag{1}$$

where $\boldsymbol{\sigma}$ is the undisturbed and $\Delta\boldsymbol{\sigma}$ the perturbed conductivity tensor, ν the electron temperature (T_e) dependent collision frequency and N_e the electron density. Assuming that the Hall- and Pedersen current density perturbations, Δj_H and Δj_P, are proportional to their respective conductivity perturbations for a given external horizontal electric field, we get

$$\Delta j_H = j_H \left(-\frac{2\,\nu}{\omega_B^2 + \nu^2}\frac{\mathrm{d}\nu}{\mathrm{d}T_e} + \frac{1}{N_e}\frac{\mathrm{d}N_e}{\mathrm{d}T_e} \right) \Delta T_e \tag{2}$$

$$\Delta j_P = j_P \left(\frac{1}{\nu}\frac{\omega_B^2 - \nu^2}{\omega_B^2 + \nu^2}\frac{\mathrm{d}\nu}{\mathrm{d}T_e} + \frac{1}{N_e}\frac{\mathrm{d}N_e}{\mathrm{d}T_e} \right) \Delta T_e , \tag{3}$$

with the electron gyrofrequency ω_B. These primary currents, which are set up in the heated region of about 25 km diameter at say 90 km, set up secondary polarization and induction currents to assure quasineutrality, as discussed by Stubbe *et al.* (1982). For frequencies well below 1 Hz the induction current can be ignored (see Fejer and Krenzien, 1982) and we use Eq. (31) of Stubbe and Kopka (1977), who included the polarization current and used height integrated conductivities, to get the angle ϕ_0 between current perturbation and ionospheric electric field. Strictly one should include the effect of magnetospheric currents (Alfvén waves) as in Eq. (14) of Glaßmeier (1984), but for large ionospheric conductivities Fejer and Krenzien (1982) showed that they were unimportant.

For frequencies > 0.5 Hz we ignore the polarization current which becomes less important as frequency increases as well as the induction current since consideration of these currents leads to serious difficulties. The consequence of the omission of the induction current is that the calculated amplitudes become larger than the measured as will be seen in the following section. We sum the Hall- and Pedersen currents with regard to their phases to give a resultant sheet current (ΔJ_H, ΔJ_P) which is then Fourier analysed. The angle ϕ_0 is subsequently calculated from :

$$\phi_0 = \arctan \frac{\Delta J_H}{\Delta J_P} . \tag{4}$$

Right- and left-hand circular rotating currents (ΔJ_R, ΔJ_L) are deduced from the Hall and Pedersen currents. The ellipticity and the sense of rotation of the resulting currents are given by :

$$\varepsilon = \frac{\Delta J_R - \Delta J_L}{\Delta J_R + \Delta J_L} \tag{5}$$

ε takes values between + 1 and − 1, corresponding to right- and left-hand circular rotation or linear if $\varepsilon = 0$.

3.2. Model calculations for November 8, 1984

A reasonable electron density profile for the model was deduced from ionograms which were taken every 5 min. The first ionogram (Fig. 12) obtained at 1600 UT, shortly before the beginning of the measurements, showed mainly echoes from the *F* layer. The minimum frequency of reflection of about 1.5 MHz, just above the electron gyrofrequency of 1.46 MHz, indicates low absorption and low ionization in the *D* region. At 1610 UT the electron density in the *E* layer begins to increase due to particle precipitation (« particle *E* »). The echoes from the *E* layer now come from lower virtual heights and extend over a growing frequency interval, until at 1630 UT the maximum critical frequency in the *E* layer is reached, corresponding to approximately $2.75 \cdot 10^{11}\ \mathrm{m}^{-3}$. For the rest of the experiment no important changes occur, the maximum density decreasing just a little.

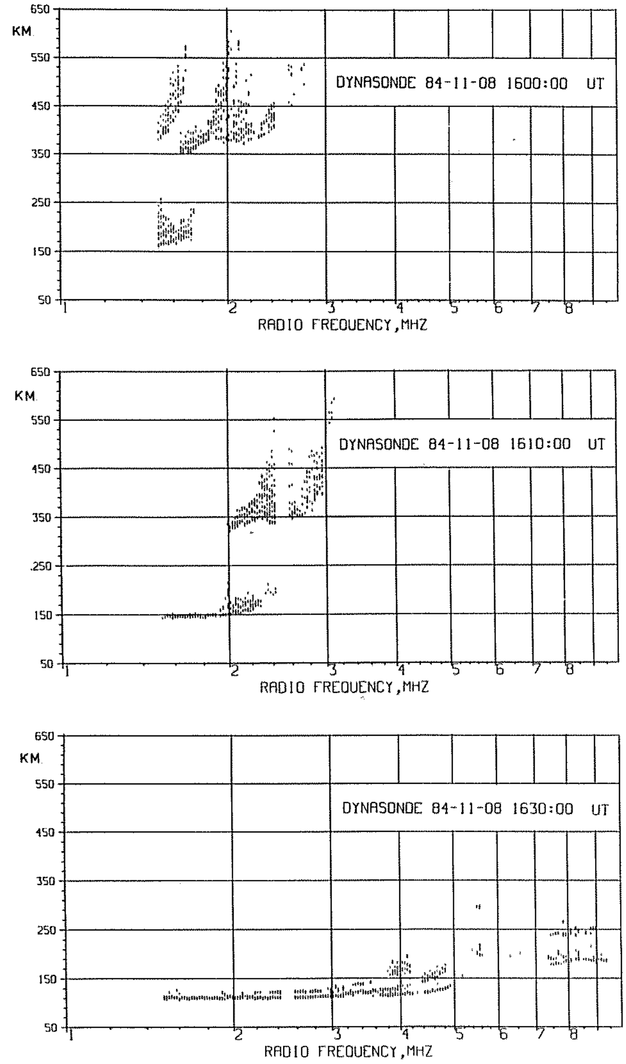

Figure 12
Three ionograms recorded at the Heating site at 1600 UT *(top),* 1610 UT *(middle), and* 1630 UT *(bottom) on November* 8.

With this information an appropriate electron density profile was chosen from Barr and Stubbe (1984) as typical for a nighttime ionosphere with low auroral activity. This profile, shown at the top right of Figure 13 was altered in one detail, so that the electron density in the E region was enhanced and was assumed to be $2.75 \cdot 10^{11}\ \mathrm{m}^{-3}$ above 110 km. Further parameters of the model are: an effective radiated power of 241 MW, a heating frequency of 2.759 MHz, a modulation frequency of 1 Hz and an ionospheric electric field of 50 mV/m, which is typical for the time interval during the experiment, as the STARE data show. In the top row the Hall (left) and Pedersen current (middle) distributions are plotted for *o*-mode heating (solid lines) and *x*-mode heating (dotted lines). The current phases, referenced with respect to the incident heating wave, are displayed below the amplitudes. The effect of density modulation can be seen to dominate above 92 km especially in the Hall current, as shown by the phase shift above this height. The resulting currents extend over a large height range because of the low electron density at low altitudes. Even so significant currents are not generated up to the height of maximum electron density because the *o*-mode is reflected at lower altitude and the *x*-mode current is negligible above 100 km. This suggests that the maximum electron density cannot be important for this experiment and this is confirmed by the magnitude and orientation of the ellipses being independent of the changes indicated by the ionograms.

The magnitudes, angles and ellipticities of the model currents are displayed in Table 4. In the case of *x*-mode heating, the Pedersen current ΔJ_P is nearly equal to the Hall current ΔJ_H so that from Eq. (4), ϕ_0 is just above 45°. For *o*-mode heating the Pedersen current is twice the Hall current because of the contribution from density modulation in the height

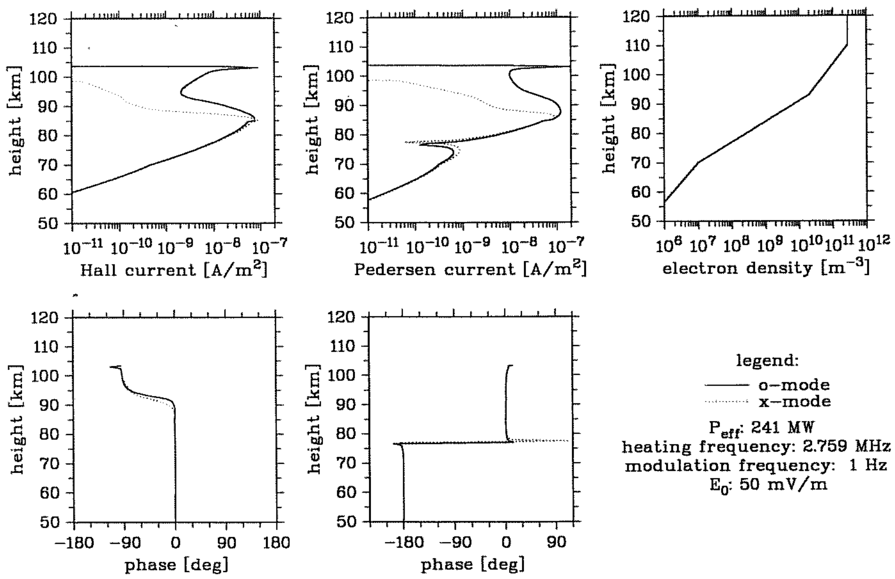

Figure 13
Results of the model calculations for the experiments on November 8. *Right plot in the top row: assumed electron density profile. Left plot in the top row: Hall currents generated by o-mode heating (solid line) and by x-mode heating (dotted line). Middle: Pedersen currents. Below the currents: phase of the current modulation relative to the radiated power. The other parameters are specified in the legend.*

Table 4
Results of the model calculations and the experiments on November 8.

Polarization	ΔJ_H [A/m^2]	ΔJ_P [A/m^2]	ϕ_0 [deg]	ϕ_0 (exp.) [deg]	ΔJ_R [A/m^2]	ΔJ_L [A/m^2]	ε	ε (exp.)
x-mode	$8.45 \cdot 10^{-7}$	$7.30 \cdot 10^{-7}$	49.2	50 ± 3	$5.62 \cdot 10^{-7}$	$5.55 \cdot 10^{-7}$	0.01	0.08 ± 0.03
o-mode	$1.07 \cdot 10^{-6}$	$2.38 \cdot 10^{-6}$	24.2	26 ± 4	$1.40 \cdot 10^{-6}$	$1.20 \cdot 10^{-6}$	0.08	0.41 ± 0.04

range of 90 to 105 km, so that ϕ_0 is considerably below 45°. The angles obtained from the experiment, which are the mean values for each mode, are subtracted from 90° to get the angle between the ionospheric electric field and the major axis of the current disturbance instead of the angle between the electric field and the major axis of the magnetic disturbance ellipse (see Fig. 7). The values show good agreement with those of the model. The right- and left-handed currents for the o-mode are larger than for the x-mode. Because the x-mode currents from higher altitudes contribute only small amounts to the total current, the phase differences due to density modulation have nearly no effect so that the polarization ellipse is linear. The case is different for o-mode heating, where significant currents are generated by density modulation at higher altitudes. The phase difference causes ΔJ_R to dominate over ΔJ_L so that the ellipticity ε is larger than zero. The experimentally determined ellipticity, deduced from the ellipses in Figure 7 which have no asterisk, are shown in the last column of Table 4. In particular the ellipticity for the o-mode deviates considerably from that determined by the model. This discrepancy could be caused by too little density modulation in the model. However the correct tendency is reproduced by the model, namely that the x-mode gives a linear polarization while the o-mode a right-handed elliptical polarization.

The magnetic field amplitudes ΔB, due to the artificial currents, can be estimated after Willis and Davis (1973) with the assumption of a homogeneous current disturbance in the heated volume using the equation

$$\Delta B = \frac{\mu_0}{4\pi z^2} V \, \Delta J \qquad (6)$$

with μ_0: permeability of the vacuum, V: heated volume, ΔJ: current disturbance. The heated volume is assumed to be a cylinder in the altitude of $z = 85$ km with a radius of $R = z \cdot \tan(14.5°/2) = 10.8$ km and a height of 5 km, since the current disturbances are centred on this altitude range as the model calculations show. Using the currents from Table 4 for x-mode heating results in $\Delta J = \sqrt{\Delta J_H^2 + \Delta J_P^2} = 1.12 \cdot 10^{-6}$ A/m^2 and a ΔB of several tens of picotesla, which overestimates the measured amplitudes by one order of magnitude. This discrepancy is probably caused by the omission of the induction current, which attenuates the primary current and — to a lesser extent — of the polarization current. Including inductive effects would only change the amplitudes significantly, but the other (polarization) parameters would remain unaffected. Fejer and Krenzien (1982) calculated a factor of 3 reduction in the calculated amplitude due to induction for 3 Hz compared to 600 s period modulation.

3.3. Model calculations for November 7, 1984

The changes of ellipse shape at the beginning of this experiment, as shown in Figure 10, are due to fast variation of the ionization in the D- and E-region as can be recognized in the ionograms which were recorded nearly every 5 min (Fig. 14). At the beginning of the experiment the absorption in the D region was extremely high because of particle precipitation resulting in almost no echoes at 1720 UT. Subsequently sporadic reflections occur at frequencies between 4 and 5 MHz, but just at 1745 UT the high ionization in low altitudes disappears and the E layer becomes visible in the ionograms. At 1750 UT a sporadic E layer remains (middle of Fig. 14), with electron density slowly decreasing with time. The last ionogram in Figure 14 reveals that the E layer critical frequencies come within measured frequency range again, corresponding to a maximum electron density of about $2 \cdot 10^{11}$ m^{-3} which is used for the following model calculations. The electron density in the E region is subject to strong changes, but the density

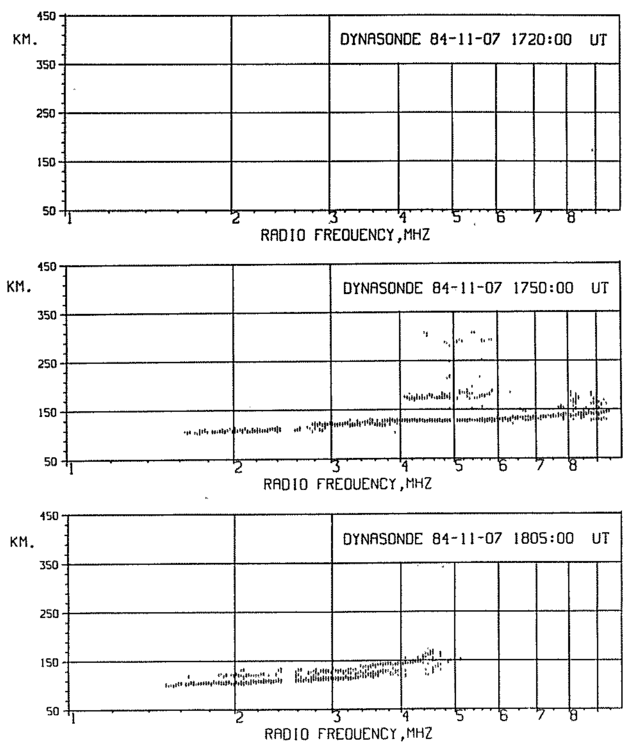

Figure 14
Three ionograms recorded at 1720 UT *(top),* 1750 UT *(middle), and* 1805 UT *(bottom) on November* 7.

profile in the D and lower E layer is more important for the artificial currents than the maximum density, because the currents due to the heating decrease strongly in the E region.

For the time interval until 1742 UT a density profile is assumed that has a well developed D layer. This profile is a modified version of profile 5 of Barr and Stubbe (1984). Changes have been made such that an electron density of $2 \cdot 10^{11}\ \mathrm{m}^{-3}$ above 110 km altitude is present as shown in Figure 15. An ionospheric electric field of 53 mV/m, that is the mean field strength in the time interval from 1721 to 1742 UT, is used for the model calculations. Because of the higher carrier frequency of 5.523 MHz (in comparison to the experiment of November 8) the heating wave reaches the E region where the currents generated by the o-mode dominate over those caused by the x-mode (see left and middle plot in the top row of Fig. 15). It can be seen from the phases that the temperature modulation prevails up to a height of 95 km, where the density modulation starts but contributes no important amount to the total current. The interesting height range is 65 to 80 km, where the phase of the Pedersen current changes. For x-mode heating the contributions to the Pedersen current from heights above and below the minimum cancel each other. For o-mode heating the contribution from altitudes above the minimum is slightly larger than that from below. Therefore the Hall current generated by the o-mode is nearly three times larger than the Pedersen current and the Hall current caused by the x-mode is approximately thirty times larger, as can be seen in Table 5. The deduced angles are 69.9° for the o-mode and 88.0° for the x-mode, which are in good agreement with the measurements (76° and 88°, respectively).

At 1748 UT the ionospheric conditions change considerably, since the electron density in the D layer decreases drastically. The mean ionospheric electric field strength is 77 mV/m between 1748 and 1804 UT. Now density profile 1 of Barr and Stubbe (1984), modified by assuming an electron density of $2 \cdot 10^{11}\ \mathrm{m}^{-3}$ above 110 km, is more appropriate. The main contributions to the total current are generated in heights above 80 km (see Fig. 16). Since the Pedersen current decreases less abruptly with height than the Hall current, the summed Pedersen current is twice the Hall current, resulting in a current flow at 26.9° to the ionospheric electric field. For the previous two modelled time intervals the density modulation had no effect for x-mode heating, and only little contribution for o-mode heating, so that the polarization is linear for the x-mode and nearly linear for the o-mode. In the last time interval the right-hand current is larger than the left-hand current because of the effect of the density modulation and hence the ellipticity deviates significantly from zero (Table 5) and is right-handed in agreement with most of the observations.

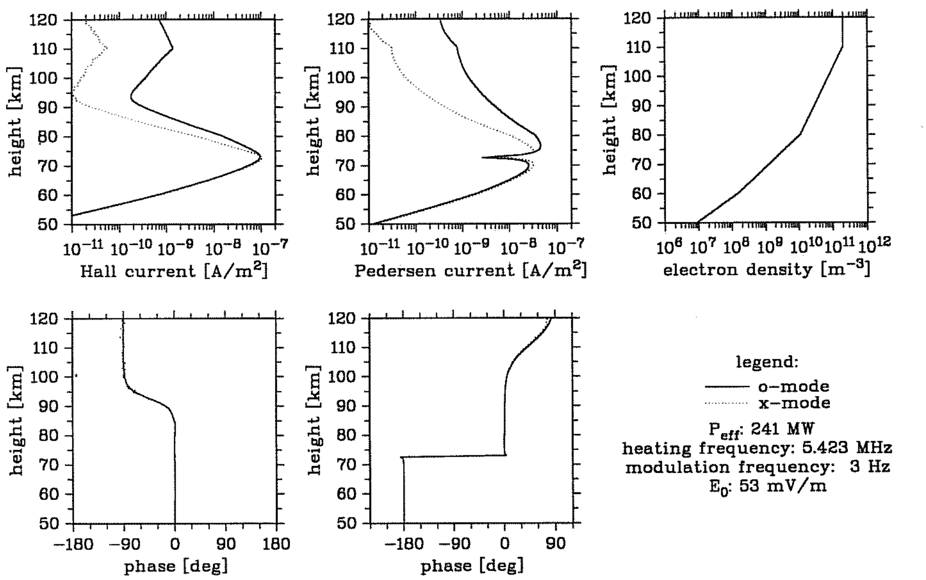

Figure 15
Results of the model calculations for the time interval between 1721 *and* 1742 UT *on November* 7 *(cf. Fig.* 9*).*

Table 5
Results of the model calculations and the experiments on November 7.

Polarization	Modelled time interval [UT]	ΔJ_H [A/m²]	ΔJ_P [A/m²]	ϕ_0 [deg]	ϕ_0 (exp.) [deg]	ΔJ_R [A/m²]	ΔJ_L [A/m²]	ε	ε (exp.)
o-mode	1721-1728	$1.56 \cdot 10^{-6}$	$5.72 \cdot 10^{-7}$	69.9	76 ± 7	$8.46 \cdot 10^{-7}$	$8.13 \cdot 10^{-7}$	0.02	0.06 ± 0.03
x-mode	1729-1742	$1.34 \cdot 10^{-6}$	$4.64 \cdot 10^{-8}$	88.0	88 ± 6	$6.71 \cdot 10^{-7}$	$6.69 \cdot 10^{-7}$	0.00	− 0.03 ± 0.05
x-mode	1748-1800	$1.64 \cdot 10^{-6}$	$3.25 \cdot 10^{-6}$	26.9	16 ± 7	$1.98 \cdot 10^{-6}$	$1.64 \cdot 10^{-6}$	0.10	0.17 ± 0.08

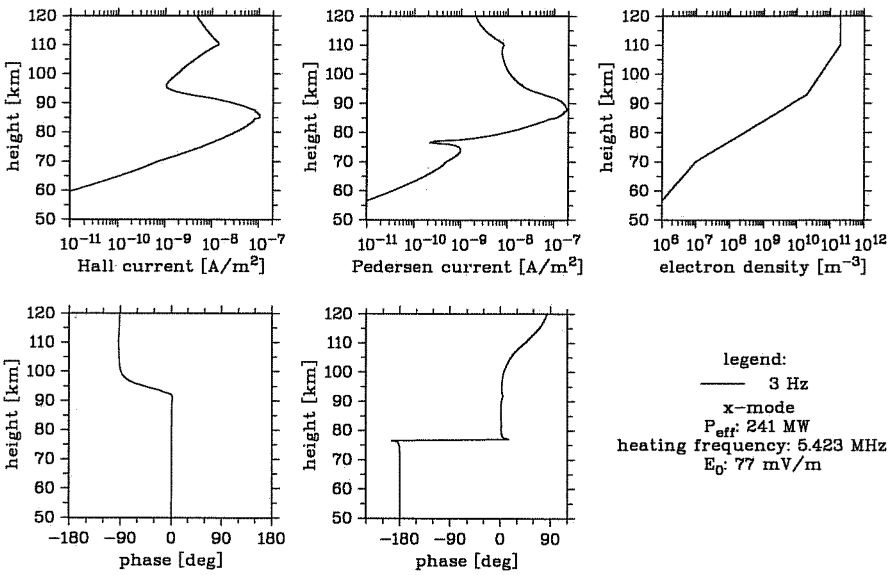

Figure 16
Results of the model calculations for the time interval between 1748 *and* 1800 UT *on November* 7 *(cf. Fig.* 9*).*

3.4. Model calculations for October 26, 1984

First we shall consider the highly variable polarization ellipses of the 1 Hz signals (middle row of Fig. 11). The findings of the previous sections suggest that the magnetic ellipse at 1859 UT is caused mainly by density modulation because it is circularly polarized.

In contrast, temperature modulation at lower heights appears to be the dominating effect at 1929 UT because of the more linear polarization. The angle ϕ_0 fluctuates between about 45° (1929 UT) and 90° (1959 UT) as the ratio of artificial Hall- to Pedersen current varies. At 1759 and 1829 UT they are comparable in magnitude so that ϕ_0 is about 45°. At 1859 UT the Hall current, due to increased density modulation, appears to increase and then decrease until they are comparable again at 1929 UT. At 1959 UT the Pedersen current appears to dominate since the ellipse is perpendicular to the electric field.

For a quantitative analysis we choose the time interval 1827 UT to 1829 UT. The density profile measured by EISCAT gives $10^{11}\ m^{-3}$ in the *E* region. The ionograms showed a minimum frequency of 1.5 MHz as well as multiple reflections of the *E* layer indicating low ionization in the *D*- and lower *E* region. We use a density of about $10^7\ m^{-3}$ below 100 km, which is also supported by the modelling of the 1425 Hz ELF waves. Using the density profile shown in Figure 17 and an ionospheric electric field of 50 mV/m measured by EISCAT at 1831 UT, we calculate the primary source currents for all three modulation frequencies (see Fig. 17). The calculated and experimental ULF perturbations are given in Table 6. The model calculations for the 120 s oscillations yield $\phi_0 = -19.1°$

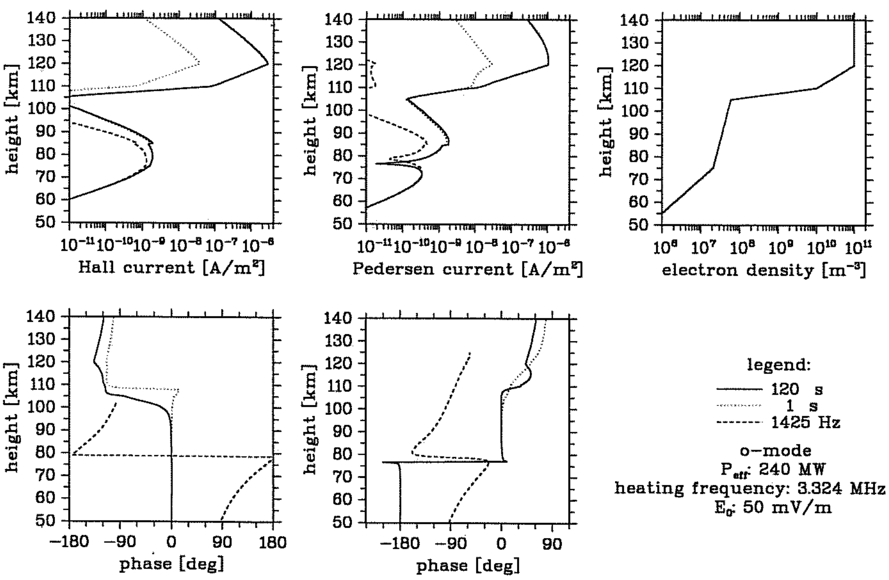

Figure 17
Results of the model calculations for the 120 s-, 1 Hz- *and* 1425 Hz-*experiments at* 1827 *and* 1829 UT *on October* 26.

Table 6
Comparison of the model calculations for the ULF *experiments with the experimental results for the instant* 1829 UT *on October* 26.

Currents, parameters	Modulation period 120 s	1 s
J_H [A/m²]	$1.71 \cdot 10^{-5}$	$1.79 \cdot 10^{-7}$
J_P [A/m²]	$4.76 \cdot 10^{-6}$	$3.03 \cdot 10^{-7}$
Σ_H [A/Vm]	4.52	—
Σ_P [A/Vm]	3.13	—
arctan (Σ_H/Σ_P) [deg]	55.3	—
arctan $(\Delta\Sigma_H/\Delta\Sigma_P)$ [deg]	74.4	—
ϕ_0 [deg]	− 19.1	30.6
ϕ_0(exp.) [deg]	− 34.1	52.9
J_R [A/m²]	$9.05 \cdot 10^{-6}$	$2.30 \cdot 10^{-7}$
J_L [A/m²]	$8.71 \cdot 10^{-6}$	$9.62 \cdot 10^{-8}$
$\varepsilon = (J_R - J_L)/(J_R + J_L)$	0.02	0.41
ε (exp.)	0.48	0.33

from Eq. (31) of Stubbe and Kopka (1977) so that the angle between major half-axis of the magnetic field ellipse and the external electric field is $(90° - \phi_0)$ or 70.9° and is in reasonable agreement with the experimentally found value of 55.9°. The model yields a low ellipticity of 0.02, whereas the measured ellipticity is 0.48. There is some uncertainty in the measured ellipticity, however, which may contain contributions from background noise since magnetometers record the disturbances integrated over a large ionospheric area but is still unlikely to explain such a large discrepancy. The magnetic field amplitude for the 120 s oscillations, using the method of Willis and Davis (1973) with the currents from Table 6 at a height of 120 km corresponding to a cylinder radius of 15.3 km, is 450 pT, only a factor of two less than the measured amplitudes. This suggests that a feedback process like that suggested by Stubbe *et al.* (1985) may not be necessary to enhance the initial perturbation if one has chosen the right electron density profile.

At 1 Hz the density modulation, which is substantially more effective than temperature modulation, is not yet fully developed, as one can see by the magnitude of the current perturbations. The artificial currents at 1 Hz and 120 s period differ by up to two orders. Hall- and Pedersen currents are of comparable magnitude for the 1 Hz modulation at 1829 UT, so that ϕ_0 is 30.6°. However, the contribution of the density modulation is large enough to change the form of the oscillation from linear to elliptical. Hence the right-handed rotating current is approximately twice the left-handed current yielding an ellipticity of 0.41 which is close to the experimentally determined value of 0.33. The modelled 1 Hz oscillations have an amplitude of 8.9 pT, a factor of 5 too large (compared to a factor 10 too large for November 8). This is again likely to be due to neglection of the induction current.

At 1425 Hz the summed Pedersen current is $9.65 \cdot 10^{-9}$ A/m² compared to a Hall current of $3.30 \cdot 10^{-8}$ A/m². For this ELF frequency, however, the wavelength now lies in the order of the vertical distance between earth and ionosphere, so the interference of the waves generated at different heights as well as reflections from the ground must be taken into account. This is done by a full wave calculation which is described in the paper of Rietveld *et al.* (1987). The calculations show that the waves excited by the Hall current disturbances dominate since the waves generated by the Pedersen current perturbations cancel each other. Consequently the major half-axes of the polarization ellipses point along the direction of the ionospheric electric field. Let β be the angle between major half-axis of the magnetic wave field and the ionospheric electric field (in contrast to the angle ϕ_0 between current disturbance and ionospheric electric field). β is determined from the phases ψ_R, ψ_L of the right- and left-handed rotating magnetic wave fields B_R and B_L according to the equation $\beta = (\psi_R - \psi_L)/2$ (cf. Rietveld *et al.*, 1987). The model yields $\beta = 29.3°$ whereas the experimentally determined angle is 11.3° (see Table 7). The amplitudes for the right- and left-handed rotating magnetic wave fields also show reasonable agreement, and the ellipticity derived from the wave amplitudes by the equation $\varepsilon = (B_R - B_L)/(B_R + B_L)$ is close to the experimentally found value.

Table 7
Comparison of the model calculations for the ELF *experiment with the experimental results for the instant* 1827 UT *on October* 26.

Magnetic wave field, parameters	Modulation frequency 1425 Hz model	experiment
B_R [pT]	0.133	0.134
B_L [pT]	0.095	0.091
ψ_R [deg]	128.2	—
ψ_L [deg]	69.7	
$\beta = (\psi_R - \psi_L)/2$ [deg]	29.3	11.3
$\varepsilon = (B_R - B_L)/(B_R + B_L)$	0.17	0.19

4. CONCLUSIONS

Three heating experiments performed in October and November 1984 under quiet and disturbed magnetic conditions and using modulation frequencies from 120 s period to 1425 Hz were presented. The amplitudes of signals in the Hz range and above generally followed the electric field in amplitude and direction, supporting the concept of current modulation as an explanation. Similar conclusions were reached by Rietveld *et al.* (1987) for the ELF/VLF range. The current modulation theory of Stubbe and Kopka (1977), where density modulation plays the most important role, reproduces the amplitude of the 120 s period oscillations quite well but overestimates the amplitudes of signals in the 0.7-10 Hz range by up to an order of magnitude. This is largely because self inductance, which is ignored, becomes important. Current modulation at kHz frequencies (where only temperature modulation is important) together with a full-wave theory reproduces amplitudes in the kHz range very well, but underestimates those in the Hz region (Rietveld *et al.*, 1989).

In the transition region between density and temperature modulation the orientation and ellipticity of the polarization ellipses could, for some cases in the Hz range, be well reproduced by a simple model in which the measured polarization parameters reflect the polarization of the modulated current system. In particular we can reproduce the predominantly right-handed polarization and the increase in ellipticity as the heater wave changes from *x*- to *o*-mode by including the contribution from electron density modulation. It was not possible to reproduce the exact values measured but that would require a more detailed model and better information on some of the ionospheric processes. For example the density modulation is treated rather simplistically. There is also some uncertainty in some of the measured polarization ellipses for low signal to noise ratios where polarized contributions from natural pulsations are superposed on the artificial signals.

Although we cannot conclude from our data that other theories which attempt to explain ULF perturbations without the presence of external electric fields, such as proposed by Kuo and Lee (1983) or Papadopoulos and Chang (1985), are not correct, we have not detected ULF perturbations under extremely quiet conditions when one might expect such mechanisms to be dominant. Significant ionospheric fields were measured by the radars during our experiments so we have shown that conductivity modulation in the presence of such fields can explain many of the features of our data without resorting to more exotic explanations.

Acknowledgements

We thank E. Nielsen for providing the STARE data, K. Schlegel for the EISCAT data and H. Lühr for the flux gate recordings of the EISCAT magnetometer cross. The Heating facility of the Max-Planck-Institut für Aeronomie was supported by the Deutsche Forschungsgemeinschaft.

REFERENCES

Barr, R., and P. Stubbe, ELF and VLF radiation from the « polar electrojet antenna », *Radio Sci.*, **19**, 1111-1122, 1984.

Barr, R., P. Stubbe, M. T. Rietveld, and H. Kopka, ELF and VLF signals radiated by the « polar electrojet antenna » : experimental results, *J. Geophys. Res.*, **91**, 4451-4459, 1986.

Fejer, J. A., and E. Krenzien, Theory of generation of ULF pulsations by ionospheric modification experiments, *J. Atmos. Terr. Phys.*, **44**, 1075-1087, 1982.

Getmantsev, G. G., A. V. Gul'el'mi, B. I. Klain, D. S. Kotik, S. M. Krylov, N. A. Mityakov, V. O. Rapoport, V. Yu. Trakhtengerts, and V. A. Troitskaya, Excitation of magnetic pulsations under the action on the ionosphere of radiation of a powerful short-wave transmitter, *Radiophys. Quantum Electron.*, **20**, 703-705, 1977.

Glaßmeier, K.-H., On the influence of ionospheres with non-uniform conductivity distribution on hydromagnetic waves, *J. Geophys.*, **54**, 125-137, 1984.

Gul'el'mi, A. V., O. D. Zotov, B. I. Klayn, N. N. Rusakov, P. P. Belyaev, D. S. Kotik, S. V. Polyakov, and V. O. Rapoport, The excitation of geomagnetic pulsations in connection with periodic heating of the ionosphere by powerful shortwave (sw) radio radiation, *Geomagn. Aeron.*, **25**, 80-83, 1985.

Gurevich, A. V., and V. V. Migulin, Investigations in the U.S.S.R. of non-linear phenomena in the ionosphere, *J. Atmos. Terr. Phys.*, **44**, 1019-1024, 1982.

Huang, C.-M., M. Whitaker, M. A. Biondi, and R. Johnsen, Electron-temperature dependence of recombination of electrons with $H_3O^+ \cdot (H_2O)_n$-series ions, *Phys. Rev. A*, **18**, 64-67, 1978.

Kuo, S. P., and M. C. Lee, Earth magnetic field fluctuations produced by filamentation instabilities of electromagnetic heater waves, *Geophys. Res. Lett.*, **10**, 979-981, 1983.

Lunnen, R. J., A. J. Ferraro, H. S. Lee, R. Allshouse, K. Carroll, and D. Werner, Detection of local and long-path VLF/ELF radiation from modulated ionospheric current systems, *Radio Sci.*, **20**, 533-563, 1985.

Papadopoulos, K., and C. L. Chang, Generation of ELF/ULF waves in the ionosphere by dynamo processes, *Geophys. Res. Lett.*, **12**, 279-282, 1985.

Rankin, D., and R. Kurtz, Statistical study of micropulsation polarizations, *J. Geophys. Res.*, **75**, 5444-5458, 1970.

Rietveld, M. T., H. Kopka, and P. Stubbe, *D*-region characteristics deduced from pulsed ionospheric heating under auroral electrojet conditions, *J. Atmos. Terr. Phys.*, **48**, 311-326, 1986.

Rietveld, M. T., H.-P. Mauelshagen, P. Stubbe, H. Kopka, and E. Nielsen, The characteristics of ionospheric heating-produced ELF/VLF waves over 32 hours, *J. Geophys. Res.*, **92**, 8707-8722, 1987.

Rietveld, M. T., P. Stubbe, and H. Kopka, On the frequency dependence of ELF/VLF waves produced by modulated ionospheric heating, *Radio Sci.*, **24**, 270-278, 1989.

Schlegel, K., M. Rietveld, and A. Maul, A modification event of the auroral *E* region as studied with EISCAT and other diagnostics, *Radio Sci.*, **22**, 1063-1072, 1987.

Stubbe, P., and H. Kopka, Modulation of the polar electrojet by powerful HF waves, *J. Geophys. Res.*, **82**, 2319-2325, 1977.

Stubbe, P., and H. Kopka, Ionospheric modification experiments in northern Scandinavia — a description of the heating project, *Report MPAE-W-02-79-04*, Max-Planck-Institut für Aeronomie, D-3411 Katlenburg-Lindau 3, FRG, 1979.

Stubbe, P., H. Kopka, M. T. Rietveld, and R. L. Dowden, ELF and VLF wave generation by modulated HF heating of the current carrying lower ionosphere, *J. Atmos. Terr. Phys.*, **44**, 1123-1135, 1982.

Stubbe, P., H. Kopka, M. T. Rietveld, A. Frey, P. Høeg, H. Kohl, E. Nielsen, G. Rose, C. LaHoz, R. Barr, H. Derblom, Å. Hedberg, B. Thidé, T. B. Jones, T. Robinson, A. Brekke, T. Hansen, and O. Holt, Ionospheric modification experiments with the Tromsø Heating Facility, *J. Atmos. Terr. Phys.*, **47**, 1151-1163, 1985.

Willis, J. W., and J. R. Davis, Radio frequency heating effects on electron density in the lower *E* region, *J. Geophys. Res.*, **78**, 5710-5717, 1973.